

## EXPERIMENTAL AND RHEOLOGICAL MODELLING ON THE STABILIZATION OF IRON ORE SLURRY USING A BIOSURFACTANT EXTRACTED FROM *ALOE BARBADENSIS* MILLER

Subrata Narayan Das<sup>1,2</sup>, Susanta K. Biswal<sup>1\*</sup>, Ajit Behera<sup>3\*</sup>, Hamza Belbsir<sup>4</sup>, Khalil El-Hami<sup>4</sup>  
and Ranjan K. Mohapatra<sup>5\*</sup>

<sup>1</sup>School of Applied Sciences, Centurion University of Technology and Management, Odisha,  
India

<sup>2</sup>Department of Mining Engineering, Government College of Engineering, Keonjhar, Odisha,  
India

<sup>3</sup>Department of Metallurgical and Materials Engineering, National Institute of Technology,  
Rourkela-769008, Odisha, India

<sup>4</sup>Mohammed V University in Rabat, Scientific institute. BP 703, Av. Ibn Batouta, Agdal, Rabat,  
Morocco

<sup>5</sup>Department of Chemistry, Government College of Engineering, Keonjhar-758002, Odisha,  
India

(Received November 8, 2023; Revised January 30, 2024; Accepted February 2, 2024)

**ABSTRACT.** The pipeline transportation of iron ore slurry (IOS) is an eco-friendly alternate mode to transport the raw materials to longer distance and reduce the transportation network congestion problems. Proper selection of surfactant could modify mineral's viscosity, dispersion and wetting characteristics effectively as may be desired, which may further be monitored. A surfactant alters surface characteristics after being adsorbed onto minerals by altering the interfacial behaviour. This work is first report of the influence of a biosurfactant sourced from *Aloe barbadensis* Miller on the rheological behaviour of a high-grade iron ore (IO) sample at 45–72% by mass slurry concentrations range. The observed rheological parameters confirmed the non-Newtonian flow behaviour of the slurry. The collected IO and dried IOS samples were subjected to UV-Vis, XRF, PSD, XRD, SEM and EDS analyses. Experimental rheological data at varying concentrations was tested on various models to ascertain the best-fit rheological model for IOS transport. The Bingham model was found to be the most suitable to model the rheology of IOS. Experimental rheological behaviour of IOS was found to be linear with the yield stress. The study shall help to ascertain the suitability of a biosurfactant to stabilise high grade iron ores for pipeline transportation.

**KEY WORDS:** Iron ore slurry, *Aloe barbadensis*, Rheological measurements, Rheological modelling

### INTRODUCTION

The iron and steel industries have grown exponentially worldwide due to huge amount of constructional activities. To meet the demand of iron ore, it is normally transported by rail and by road (truck and lorry) which causes serious environmental pollutions for particulate matters [1, 2]. Transporting the iron ore by rail is cost effective as compared to road transportation. The railway lines are not well connected with the mining areas as most of the iron deposits are hilly deposits. So, first the iron ore is transported by trucks from such remote areas to nearby railway siding for rail transportation which add extra transportation cost. The road transportation is not environmentally friendly and also chances of spillage of iron ore is more. So, most of the industries not preferring to transport through road. Moreover, the rate of accident is more due to road transportation through trucks and lorries as such vehicles run in township crowded areas. To overcome such congested transportation networks and adopting an economic and environmentally

\*Corresponding author. E-mail: [ranjank\\_mohapatra@yahoo.com](mailto:ranjank_mohapatra@yahoo.com) (R.K. Mohapatra); [dr.skbiswal@cutm.ac.in](mailto:dr.skbiswal@cutm.ac.in) (S.K. Biswal); [beheraajit@nitrrkl.ac.in](mailto:beheraajit@nitrrkl.ac.in) (A. Behera)

This work is licensed under the Creative Commons Attribution 4.0 International License

friendly transportation system, the iron ore is now transported through pipelines in form of slurries and some more industries have ambitious future plans for installing such iron ore slurry pipelines [1, 3].

Slurry flow is usually done to transport solid particles with liquid (mostly water) as a carrier fluid. The slurry mixture is normally pumped by a device known as centrifugal pump. The size of solid particles varies between 1-100mm. Slurry flow in pipelines is different from the single phase flow. For smooth flow of slurry and also to pump easily the physical characteristics of slurry are responsible and which are dependent on many factors such as concentration of solids in liquid phase, size and distribution of particles, and viscosity of the carrier [4]. The viscosity of the slurry increases during the attainment of slurry with high solid concentration because of the increase in particle-particle interaction. This will affect power requirements for pumping during its aqueous transportation through pipeline [5]. Moreover, the country's economy is also strongly influenced by the mining activities. So, special importance is highly recommended on rapid and inexpensive means for formulating and stabilising the slurry and to minimize the power requirements and increase energy sustainability [6]. Surfactants are amphiphilic in nature and have the unique property to reduce the surface tension when mixed with water. For the stabilization of different slurries, normally commercial surfactants (sodium dodecyl sulphate, cetyl trimethyl ammonium bromide, etc.) are used. Bioadditives, as a futuristic intervention, reportedly positively impacted the rheology of IOS. Stabilising a slurry using natural surfactants is an ecofriendly, pollution-free and cost effective approach and essential for a sustainable biosystem [7, 8]. The stability and rheological behaviour of ore-water slurry (OWS) potentially can ease the transportation.

Biosurfactants extracted from *Acacia concinna*, *Sapindus laurifolia*, *Acacia auriculiformis*, etc. have also been successively tried in fly ash and coal slurry stabilisation [9-15]. Gupta and Kumar studied the stability and flow of IOS using surfactant (*Sapindus mukorossi* and sodium dodecyl sulfate) mixed system [16]. Behari and coworkers investigated the rheological characteristics of IOS using a natural surfactant from *Sapindus laurifolia fruits* [17]. They also used *Acacia concinna* fruit extract as a IOS surfactant [18]. Das and coworkers formulated and stabilised highly concentrated IOS using a natural surfactant from *Colocasia esculenta* (L.) Schott leaf [19]. This is an eco-friendly, cost effective and economical way to transport IO. A study also suggested that the saponin molecules from aqueous *Acacia auriculiformis* coated well on the iron surface and formed an effective barrier between the iron ore particles to stabilise high grade IOS [20].

This work is an account of the rheological behaviour studies on a high grade IO sample in a slurry concentration range of 45–72% by mass with a biosurfactant extracted from *Aloe barbadensis* Miller. The gel extracted from *Aloe barbadensis* Miller leaf has pharmacological and cosmetic applications. Therapeutic (anticancer, antidiabetic, antioxidant and antihyperlipidemic) benefits of *Aloe vera* gel was reported [21]. However, this work reports its application in IOS stabilisation for the first time.

## EXPERIMENTAL

### *Preparation of IO sample*

The lump IO was obtained from Jindal Steel, Joda of Keonjhar district of Odisha, India. The sample was crushed and powdered by using Jaw crusher (Testmaster) and ball mill in the mineral engineering laboratory of the Government College of Engineering, Keonjhar. The sample was sieved to various sizes (-38, +38-63 and +63-75  $\mu\text{m}$ ) using standard sieve (Micon engineers).

### *Preparation of aqueous extract of Aloe vera*

*Aloe barbadensis* Miller (*Aloe vera*) of the genus *Aloe* is cosmopolitan in distribution, found worldwide mainly in the dry regions of Asia, Africa, Europe and America. The skin of *Aloe vera*

leaf has high saponin content compared to other parts [22]. For the aqueous extract of saponin (surfactant), 100 g of dried leaf was powdered and dissolved in 1 L water with constant stirring for 2 h using a magnetic stirrer. The preparation was filtered to extract the active component.

#### *Surface activity of the surfactant*

The surface activity of the aqueous *Aloe vera* extract was investigated using surface tensiometer. The surface tension reduced steadily till critical micellar concentration (CMC) was reached with increasing surfactant concentration. The CMC of *Aloe vera* with and without IO was analysed.

#### *Rheological behaviour measurement*

The desired slurry concentration was prepared in a beaker having aqueous *Aloe vera* solution adding IO powder in installments and stirring for 20 min. The rheology of IOS (45–72% concentration range) was estimated using HAAKE RheoStress 1 (ThermoFisher Scientific) rheometer at room temperature. About 30 mL of IOS sample was taken in a clean rheology cup with controlled shear rates (0-300/s) at 30 °C to estimate the rheology.

#### *Methods*

The chemical composition of the samples were analysed using a XRF (Zentium, Malvern Panalytical) instrument. Particle size distribution was measured using a Malvern Mastersizer (Malvern, UK) instrument. X-Ray diffraction analysis was done using a Bruker D8 advance XRD system. The surface morphology was SEM and EDS analysed using a JEOL JSM-6480LV scanning electron microscope [19, 20].

## RESULTS AND DISCUSSION

#### *X-Ray fluorescence (XRF) study*

XRF analysis showed that the major component of the IO sample was hematite ( $\text{Fe}_2\text{O}_3$ ), with little amount of silica ( $\text{SiO}_2$ ), alumina ( $\text{Al}_2\text{O}_3$ ),  $\text{P}_2\text{O}_5$ , CaO and others. As per the generated data, the percent weight of  $\text{Fe}_2\text{O}_3$  slightly increased from 96.77% to 97.63% with *Aloe vera* treatment [20]. Similar trend also observed for  $\text{Al}_2\text{O}_3$ , attributable to the iron and aluminium present in *Aloe vera* gel [23].

#### *Particle size analysis*

Particle size distribution of IO samples was measured using Malvern Mastersizer instrument (Malvern Instruments Ltd. UK). As per the observed data, the mean diameter of IO-sample before *Aloe vera* treatment was 8.11  $\mu\text{m}$  with a specific surface area of 0.2633  $\text{m}^2\text{g}^{-1}$ . The particle size slightly increases after *Aloe vera* treatment. The mean diameter of IO-sample after *Aloe vera* treatment was 9.25  $\mu\text{m}$  with 0.2661  $\text{m}^2\text{g}^{-1}$  specific surface area.

#### *Surface morphology (SEM and EDS)*

The surface morphology of the samples was imaged (Figure 1) which showed a well-formed structure, shape and texture of IO-sample before (Figure 1a) and after (Figure 1b) the surfactant treatment with visible gains at microscales. SEM images showed widely distributed ornamental and lacy grains of varying shape. As per the natures of microstructures, the grains aggregated as dense-packs over the sample surface. The nature of the grains observed in the micrographs was

polycrystalline as the grain aggregates formed larger agglomerates with dense domain [19, 20]. There was no change in the grains after adding the surfactant to IO-sample. The aggregates could be specified and measured in numerous ways. Gwyddion line profile was used to statistically calculate the average of dimensions of the grains (Figure 1c) to the plotted ones (Figure 1d). The grains had different shapes with the size varying in width (between 0.2  $\mu\text{m}$  and 2  $\mu\text{m}$ ) and length (between 2  $\mu\text{m}$  and 6  $\mu\text{m}$ ).

Based on the XRD pattern obtained, the presence of 67.24% iron and 18.26% oxygen was confirmed with varying iron oxide type/phase. Zirconium present along with major elements could be due to the added *Aloe barbadensis* Miller surfactant extract.

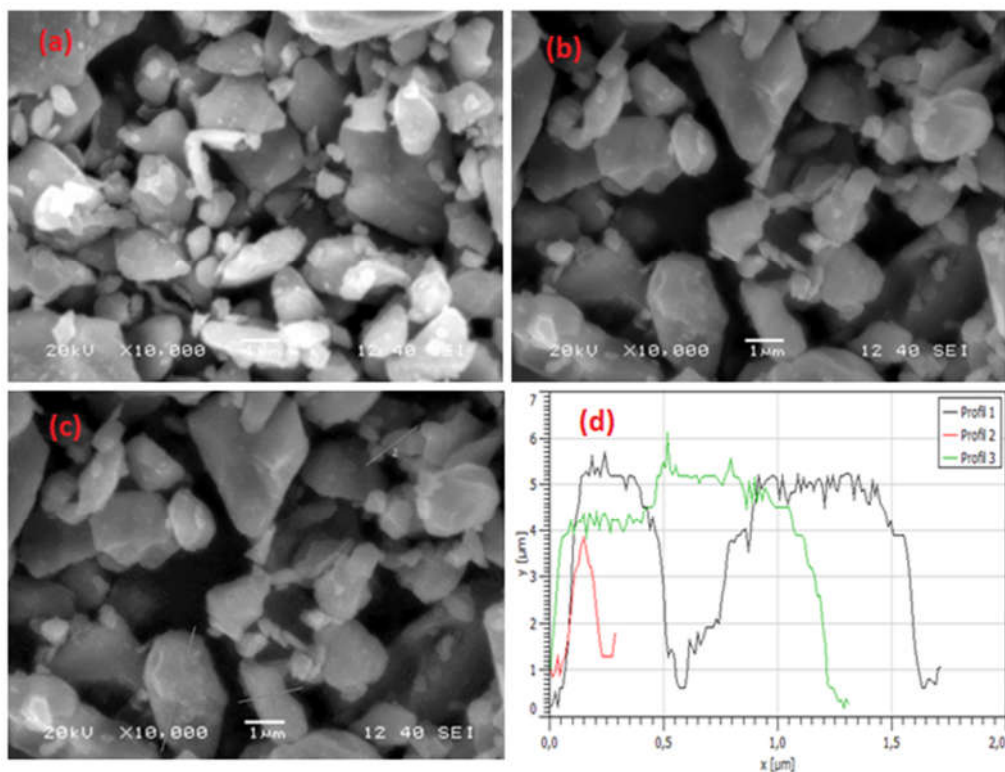


Figure 1. SEM images of iron ore particles (a: IO-sample, b: IO after *Aloe vera* treatment, and c, d: calculated Gwyddion line profile).

#### *XRD study*

Figure 2 depicts the XRD patterns of IO and the surfactant treated iron ore at room temperature. Fine and intense peaks suggest structural order in the samples with the existence of crystalline regions. Surfactants were found to facilitate crystallization of metastable forms in earlier studies [19, 20]. XRD pattern showed rhombohedral crystal structure with R-3c space group. The lattice parameters for the selected unit cell presented in Table 1 were refined using X'pert High score Software (#JCPDS 01-089-0596 and 00-024-0072).

Approximate size of crystallite ( $P$ ) was calculated using Scherer's equation,  $P = K\lambda/\beta_{1/2}\cos\theta hkl$ , where  $K$  (dimensionless shape factor) is 0.89,  $\beta_{1/2}$  = peak width of the broadening

line of XRD peak at half of the intensity and  $\lambda =$  X-Ray wavelength of 1.5405 Å. The average P values were determined as 31 and 37 nm. Surfactant addition to IO increased the crystallite size as compared to iron ore without surfactant addition. It is explained by improved solubility and crystallisation due to the applied anti-solvent in presence of surfactant. Microstructure parameters like micro strain and dislocation density were determined with XRD broadening analysis. The micro strain and dislocation density values confirmed the presence of less number of lattice defects (Table 1).

Table 1. Lattice and structural parameters of the samples.

Samples	a = b (Å)	c (Å)	Crystallite size (nm)	Dislocation density (nm <sup>-2</sup> )	Microstrain (ε)
Iron ore sample	5.6916	13.722	31.7	0.0013205	0.0025
Iron ore after the treatment with surfactant	5.8656	13.710	37.4	0.001391	0.002022

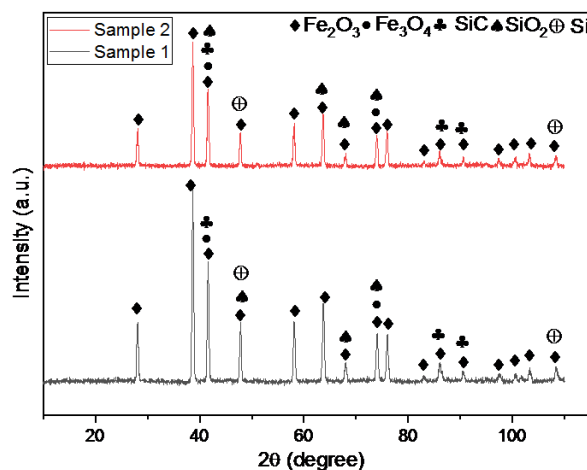


Figure 2. XRD of iron ore slurry sample (sample-1: before the treatment with surfactant and sample-2: after the treatment with surfactant).

### Electronic spectra

The electronic spectra of the iron powder samples both before and after the addition of surfactant were obtained using double beam UV-Vis spectrophotometer (Systronics) in DMSO (Figure 3a). Comparing both the spectra, the peak position was same and the intensity differed. The peak position was same as both contained iron oxide. However, the surfactant-added iron powder displayed a more intense peak, attributed to the increased solubility of iron. The intensity of absorption is directly proportional to concentration. It clearly indicated that *Aloe vera* surfactant maximised the iron particle solubilisation and stabilised the slurry.

The electronic spectra for the aqueous extract of *Aloe vera* and the same that was released after the IO settled in the slurry were taken (Figure 3b,c). This confirmed that the absorption intensity decreased when the aqueous extract of surfactant was added to the IO sample, as the surfactant molecule coated on the surface of the IO particles.

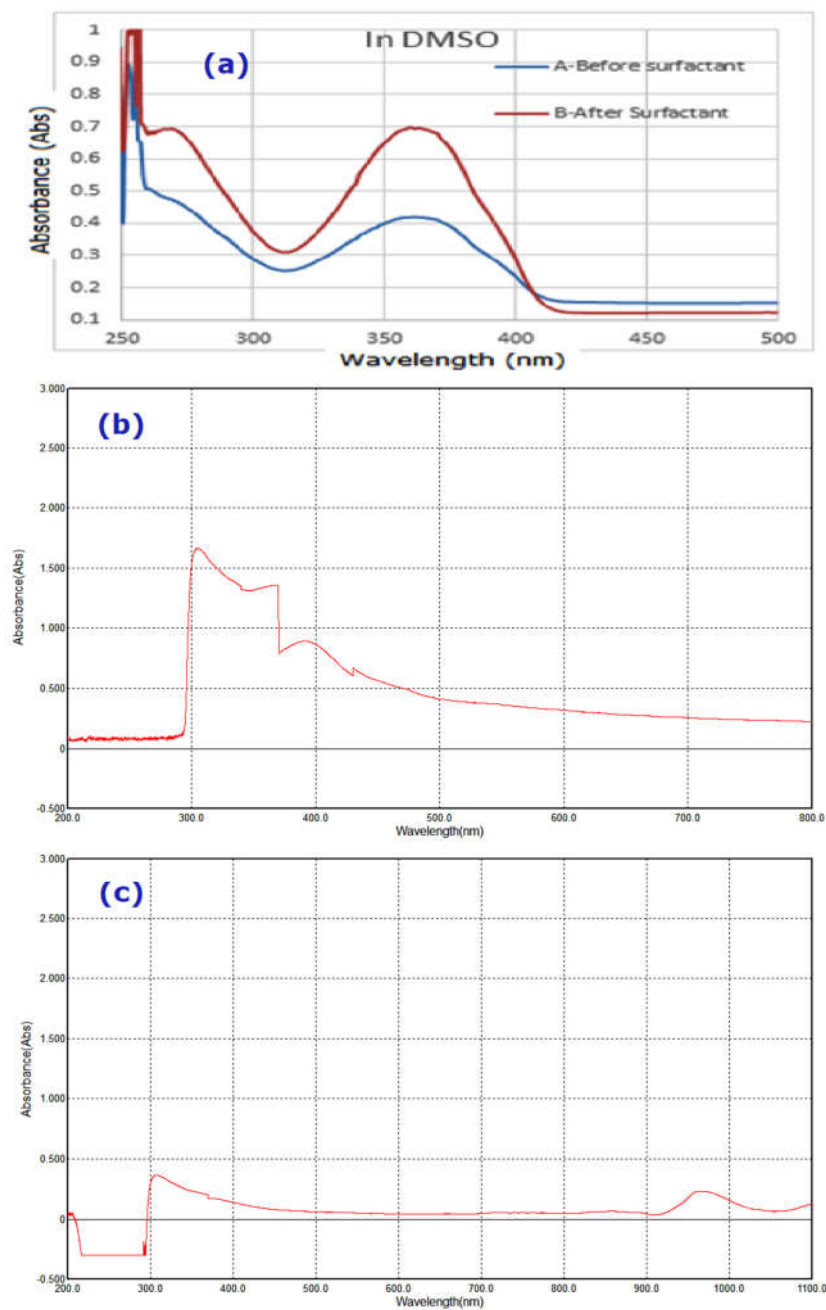


Figure 3. UV-Vis spectra of a) aqueous extract of iron powder before the addition of surfactant, b) aqueous extract of iron powder after the addition of *Aloe vera* surfactant, and c) IOS after settling.

### Rheological measurements

#### *Effect of Aloe vera concentration on the surface tension*

Surfactant reduces the surface tension of the fluids and ultimately increases the wettability in a slurry system [8-11,19,20]. The nature of a surfactant adsorbed on the solid surface stabilises the slurry. This also reduces the solid particle agglomeration to stabilise the slurry. As per the study, the surface tension decreased with increase in *Aloe vera* concentration in IOS. The surface tension was the lowest at 0.10 g/cc of *Aloe vera* (Figure 4). However, the surface tension of IOS increased with increasing iron ore concentration due to an increased interfacial surface.

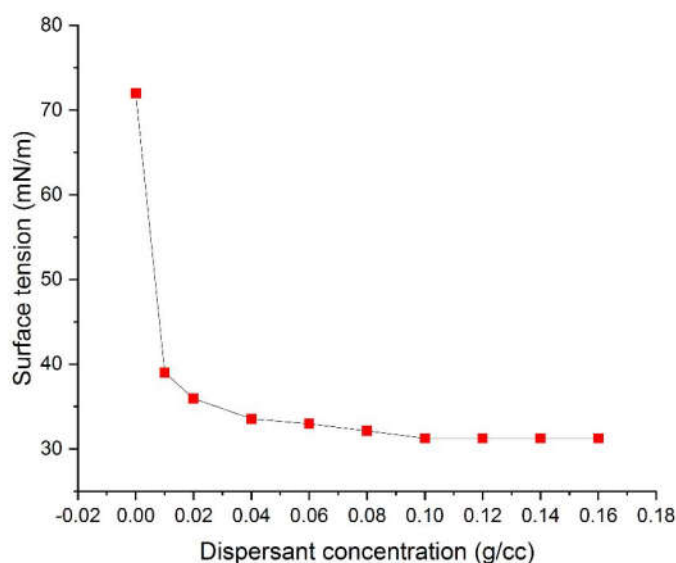


Figure 4. Surface tension vs *Aloe vera* concentration.

#### *Effect of Aloe vera concentration on apparent viscosity*

Figure 5 shows the effect of *Aloe vera* concentration (0.001–0.017 g/cc range) on the apparent viscosity of IOS. As per the plot, the viscosity of IOS significantly reduced by adding *Aloe vera*. The *Aloe vera* molecules coated on the surface of the IO particles resulting in dispersion due to the formation of effective barrier between IO particles. With increasing *Aloe vera* concentration, viscosity reduced from about 1350 to about 620 mPa.s, and no further substantial viscosity reduction was observed thereafter (Figure 5).

#### *Effect of iron ore concentration on the apparent viscosity*

The apparent viscosity of IOS (Figure 6) increases with increasing IO concentration (62-70% by weight). The apparent viscosity of IOS is essential for its pipeline transportation. The viscosity of IOS increased with increasing iron amount loading due to agglomerating solid particle at higher concentration. As per graph, the apparent viscosity gradually increased with increasing iron ore

concentration [19]. The apparent viscosity suddenly rose above 64% iron concentration and reached 745 mPa.s at 72% after which it was not suitable for pipeline transport due to iron ore particle agglomeration. The graph also suggests that a solid content between 45% and 64% possessed good fluidity. However, due to high viscosity, the fluidity decreased as iron content increased.

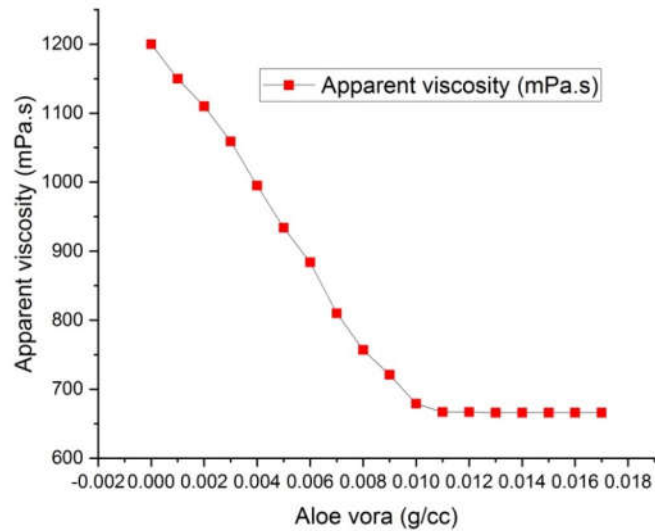


Figure 5. Effect of *Aloe vera* concentration on apparent viscosity.

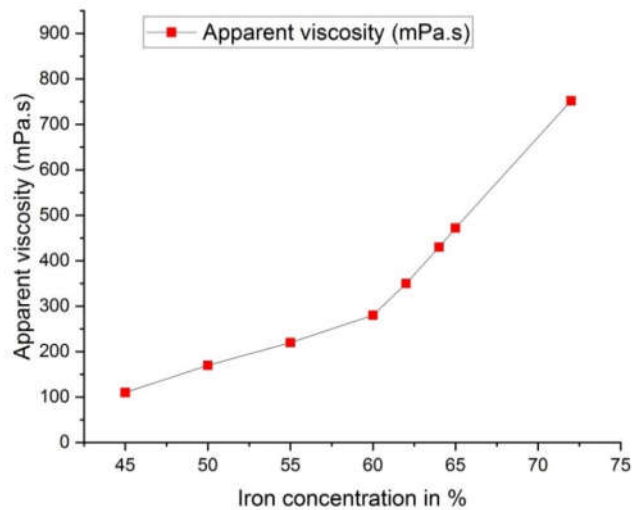


Figure 6. Effect of iron ore concentration on apparent viscosity.



### Effect of temperature on the apparent viscosity

The effect of temperature in a varying range of 298-313K on the apparent viscosity of IOS at 60% concentration was studied. The apparent viscosity decreases with rising temperature [17-20]. The kinetic energy increases with a rise in temperature, which reduces the cohesive force among the particles. Arrhenius expression describing a relationship between viscosity and temperature is:

$\ln \eta = \ln A + \frac{E}{RT}$ , where,  $\eta$  = the viscosity at a particular shear rate, A = fitting parameter, E = activation energy, T = temperature in kelvin, and R = universal gas constant.

### Rheological behaviour of IOS

It is important to study the flow behaviour of slurry for pipeline transportation. The shear stress and shear rate were studied at varying (60% and 70%) iron ore concentrations. The rheology was determined at optimised *Aloe vera* concentration. A straight line passing through the origin is obtained in the shear stress  $V_s$  shear rate plot for very low slurry concentration. The applied shear rate must overcome the yield stress for a free-flowing slurry. The IOS displayed a linear relation between shear stress and shear rate with *Aloe vera* after an early shear yield stress point, indicating a non-Newtonian Bingham plastic model obeying the equation:  $\tau = \tau_0 + \gamma\eta$ , where  $\tau$  = shear stress,  $\gamma$  = applied shear rate,  $\tau_0$  = yield stress, and  $\eta$  = the Bingham viscosity. It is confirmed from the plot that the yield stress value increased significantly with increasing IO concentration in the slurry due to agglomeration of iron ore particles at high concentration [17-20].

### Effect of shear rate on apparent viscosity

As the shear rate controls the apparent viscosity, it is essential to understand the effect of shear rate on the apparent viscosity of iron ore slurry for economical pipeline transportation [17-20]. Figure 7 showed the variation of shear rate (10 to 200  $s^{-1}$ ) with apparent viscosity of the slurry of IO concentration (60% and 70%). The plot indicated that the apparent viscosity of IOS decreased with a rise in shear rate. Slurry with 60% IO concentration showed the lowest apparent viscosity in the studied shear rates range, and hence may be economical for pipeline transportation.

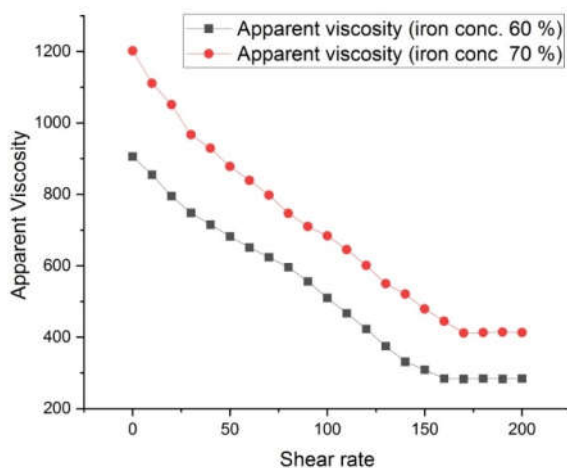


Figure 7. Effect of shear rate on apparent viscosity.

*Rheological modelling (empirical rheological models)*

The rheological modelling allows to identify the dynamic viscosity and the yield stress of IOS which can be done through the regression of experimental data (shear stress vs shear rate) to the following empirical models [24-28].

*Casson model.* The rheological behaviour of the concentrated IO suspensions with pseudoplastic behaviour may be explained with the help of the Casson model:  $\sigma^{1/2} = (a \cdot \gamma)^{1/2} + b$ , where  $\nu = a$  is the dynamic viscosity,  $b^2 =$  the yield stress,  $\gamma =$  the shear rate, and  $\sigma =$  the shear stress.

*Bingham model.* The Bingham model describes the behaviour of the iron ore suspensions with linear rheological profiles with a yield stress:  $\sigma = a \cdot \gamma + b$ , where  $a =$  the dynamic viscosity, and  $b =$  the yield stress.

*Ostwald-Power Law model.* The Ostwald model describes the rheological behaviour of IO suspensions with a dilatant profile or a pseudoplastic without yield:  $\sigma = a \cdot \gamma^n$ , where  $n =$  behaviour index of the flow, and  $a =$  the coherence parameter.

*Herschel-Buckley model.* The Herschel-Buckley model presents a generalisation of all the above cited rheological models:  $\sigma = a \cdot \gamma^p + b$ , where  $p =$  an exponent,  $a =$  dynamic viscosity related to Herschel-Buckley model, and  $b =$  the yield stress. The rheological data was fitted to the above four models to identify the best-fit rheological model to describe the experimental data at each concentration index.

*Comparison of empirical rheological models.* Regression parameters resulting from the modelling study of IOS (60% and 70% concentrations) as per the four models are shown in Tables 3 and 4. 'a' and 'b' are the viscosity and yield stress 'elasticity' for each model, whereas 'n' and 'p' are the exponents of the Ostwald and Herschel-Buckley models. It was clearly noticed from Figures 8 and 9 that the Bingham and Herschel-Buckley models are the most suitable to describe rheological behaviour of IOS. For these models, the trend curves pass through the maximum of experimental points and the  $R^2$  are close to 1 [11].

Casson and power law models were not suitable to describe IOS rheological behaviour as they had  $R^2$  far from 1. The experimental rheological behaviour of IOS was linear with the yield stress (Bingham). So the most suitable model for rheology modelling of IOS is the Bingham model [11]. So the viscosities and yield stress values generated by Bingham's law were considered.

*Mechanism to stabilise the slurry*

Metal oxides are usually insoluble in water, however few metal oxides may be sparingly soluble [19]. As reported, the surface of anhydrous hematite is slightly hydrophobic at natural pH and the hematite surface becomes hydrophilic when hydroxylation occurs at alkaline pH [29]. The hydrophobicity of the surface was observed to restore by heating at 60 °C. Surfactants (saponins) are naturally amphiphilic, and due this, the hydrophilic part orientat towards the water molecules and the hydrophobic part away from in an aqueous solution which reduced the surface tension of water and enhance the surface activity [30]. In the present study, the IO powder was sparingly soluble in water. However when aqueous extract of *Aloe vera* was added the solubility of IO increased as confirmed from UV-Vis spectra. The ESP analysis suggested that the surfactant surface was divided into two parts (hydrophilic and hydrophobic). It suggested that hydrophilic part of the surfactant was attached to the IO particle surface [31] resulting in a greater solubility due to its micellisation behaviour.

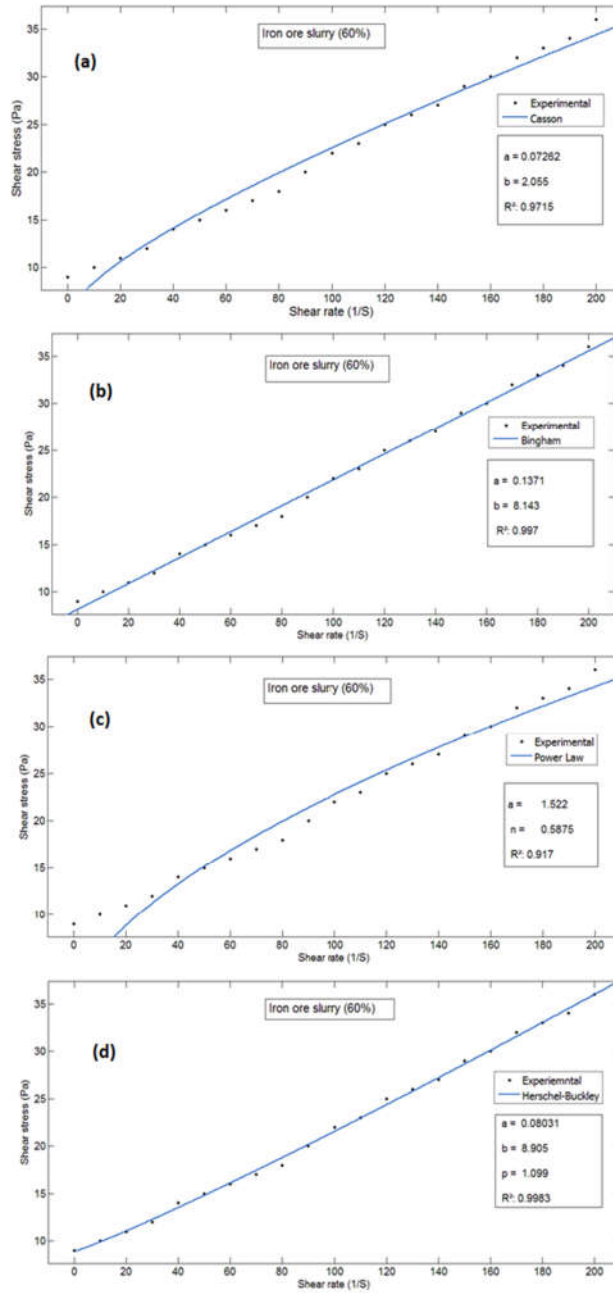


Figure 8. The fitted rheological data (at 60% IOS concentration), a) Casson model  $\sigma^{1/2} = (0.07262 \cdot \dot{\gamma})^{1/2} + 2.055$ ; b) Bingham model  $\sigma = 0.1371 \cdot \dot{\gamma} + 8.143$ ; c) Ostwald model  $\sigma = 1.522 \cdot \dot{\gamma}^{0.5875}$ ; d) Herschel-Buckley  $\sigma = 0.08031 \cdot \dot{\gamma}^{1.099} + 8.905$ .

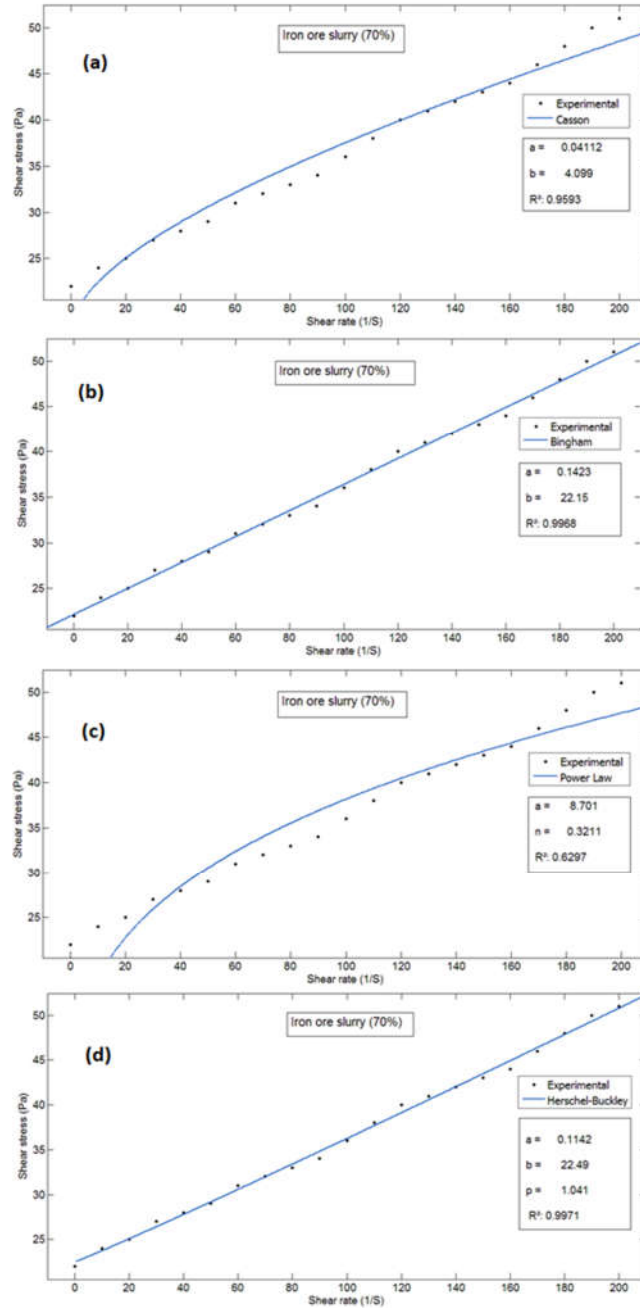


Figure 9. The fitted rheological data (at 70% IOS concentration), a) Casson model  $\sigma^{1/2} = (0.04112 \cdot \dot{\gamma})^{1/2} + 4.099$ ; b) Bingham model  $\sigma = 0.1423 \cdot \dot{\gamma} + 22.15$ ; c) Ostwald model  $\sigma = 8.701 \cdot \dot{\gamma}^{0.3211}$ ; d) Herschel-Buckley  $\sigma = 0.1142 \cdot \dot{\gamma}^{1.041} + 2.249$ .

## CONCLUSION

The rheological behaviour of high grade IOS with 45–72% concentration range by mass was investigated by stabilising it with a natural surfactant extracted from *Aloe vera*. *Aloe vera* aqueous extract enhanced the solubility of IOS. Results suggested that the biosurfactant reduced the viscosity of high concentration high grade IOS as the surfactant molecules coated well on the IO particle surface. The results of UV-Vis, XRF, PSD and XRD analyses also matches with the findings. The observed rheological parameters indicated non-Newtonian flow behaviour of IOS. Pipeline transport of IOS stabilised by *Aloe vera* aqueous extract is an economic and eco-friendly alternative that will help address the congested transportation issue. It reduces power needs. As the iron and steel industries have grown dramatically in the last few decades, further studies are recommended to bring the finding of the study to practicable operation. This work reported the application *Aloe vera* for the first time in IOS stabilisation, adding another dimension to the wide range of applications of *Aloe vera*. In the study, the *Aloe vera* significantly reduced the viscosity of IOS. This may reduce power consumption and water loss in pipeline transportation of slurry. A case study using *Aloe vera* aqueous extract is recommended to validate the findings. This study will help slurry stabilisation researchers to find possible similar use in coal, coal ash, etc.

## ACKNOWLEDGMENTS

All authors acknowledge their respective universities.

## REFERENCES

1. Das, S.N.; Biswal, S.K.; Mohapatra, R.K. Recent advances on stabilization and rheological behaviour of iron ore slurry for economic pipeline transportation. *Mater. Today: Proc.* **2020**, *33*, 5093-5097.
2. Mohapatra, R.K.; Das, P.K.; Sharun, K.; Tiwari, R.; Mohapatra, S.R.; Mohapatra, P.K.; Behera, A.; Acharyya, T.; Kandi, V.; Zahan, K.-E.; Natesan, S.; Bilal, M.; Dhama, K. Negative and positive environmental perspective of COVID-19: Air, water, wastewater, forest, and noise quality. *Egypt. J. Basic Appl. Sci.* **2021**, *8*, 364-384.
3. Indian Burro of Mines, Government of India Ministry of Mines, Slurry transportation in Indian mines, **2001**. <https://ibm.gov.in/writereaddata/files/10072016172218slurry%20pdf.pdf> (accessed on 21-11-22).
4. Senapati, P.K.; Pothal, J.K.; Barik, R.; Kumar, R.; Bhatnagar, S.K. Effect of particle size, blend ratio and some selective bio-additives on rheological behaviour of high-concentration iron ore slurry, in Paste 2018 Jewell, R.J.; Fourie, A.B. (Eds), Proceedings of the 21st International Seminar on Paste and Thickened Tailings, Australian Centre for Geomechanics, Perth, **2018**, 227-238.
5. Jennings Jr., H.Y. Transporting iron ore slurries, United States Patent, Appl. No.: 655,355, Filed: Feb. 5, **1976**.
6. Macía, Y.M.; Pedrera, J.; Castro, M.T.; Vilalta, G. Analysis of energy sustainability in ore slurry pumping transport systems. *Sustainability*. **2019**, *11*, 3191.
7. Das, D.; Sarangi, A.K.; Mohapatra, R.K.; Parhi, P.K.; Mahal, A.; Sahu, R.; Zahan, K.-E. Aqueous extract of Shikakai; a green solvent for deoximation reaction: Mechanistic approach from experimental to theoretical. *J. Mol. Liq.* **2020**, *309*, 113133.
8. Das, D.; Das, S.K.; Parhi, P.K.; Dan, A.K.; Mishra, S.; Misra, P.K. Green strategies in formulating, stabilizing and pipeline transportation of coal water slurry in the framework of Water-Energy Nexus: A state of the art review. *Energy Nexus* **2021**, *4*, 100025.

9. Das, D.; Pattanaik, S.; Parhi, P.K.; Mohapatra, R.K.; Jyothi, R.K.; Lee, J.-Y.; Kim, H.I. Stabilization and rheological behavior of fly ash–water slurry using a natural dispersant in pipeline transportation. *ACS Omega* **2019**, *4*, 21604-21611.
10. Routray, A.; Senapati, P.K.; Padhy, M.; Das, D.; Mohapatra, R.K. Effect of mixture of a non-ionic and a cationic surfactant for preparation of stabilized high concentration coal water slurry. *Int. J. Coal Prep. Util.* **2022**, *42*, 925-940.
11. Das, D.; Mohapatra, R.K.; Belbsir, H.; Routray, A.; Parhi, P.K.; El-Hami, K. Combined effect of natural dispersant and a stabilizer in formulation of high concentration coal water slurry: Experimental and rheological modelling. *J. Mol. Liq.* **2020**, *320*, 114441.
12. Mohapatra, R.K.; Das, P.K.; Kabiraz, D.C.; Das, D.; Behera, A.; Zahan, K-E. Generation, transportation and utilization of indian coal ash, Chapter: 11, Clean Coal Technologies, Jyothi, R.K.; Parhi, P.K. (Eds.), **2021**, 267–288. DOI: 10.1007/978-3-030-68502-7\_11
13. Das, D.; Kar, P.; Das, B.R.; Mohapatra, R.K.; Das, S.N.; Parhi, P.K.; Behera, U. Natural Dispersant in Coal Water Slurry Stabilization, Chapter: 2, (Clean Coal Technologies, Jyothi, R.K.; Parhi, P.K. (Eds.)), **2021**, 39-57. DOI: 10.1007/978-3-030-68502-7\_2
14. Mohapatra, R.K.; Das, D.; Behera, U.; Das, S.N.; Mohanty, A.; Mahal, A.; El-ajaily, M.M. Generation of Fly ash and Its Surface Modification for Pipeline Transportation, Chapter: 5, (Chemical Modification of Solid Surfaces by the Use of Additives, edited by R.K. Mohapatra, D. Das, M. Azam). **2021**, 94-109. DOI: 10.2174/9789815036817121010008
15. Routray, A.; Kar, P.; Nayak, N.; Mohapatra, R.K.; Mustakim, S. M.; Das, D. Improvement in the Flow Behavior of Coal–Water Slurry Using Surfactant Mixture, Chapter: 3, (Chemical Modification of Solid Surfaces by the Use of Additives, edited by R.K. Mohapatra, D. Das, M. Azam). **2021**, 44-59.
16. Gupta, C.; Kumar, S. Characterization and stabilization of iron ore suspension and influence of the mixture of natural additive Sapindus mukorossi and SDS on the slurryability, *J. Disper. Sci. Technol.* **2023**, DOI: 10.1080/01932691.2023.2212752
17. Behari, M.; Mohanty, A.M.; Das, D. Influence of a plant-based surfactant on improving the stability of iron ore particles for dispersion and pipeline transportation. *Powder Technol.* **2022**, *407*, 117620.
18. Behari, M.; Mohanty, A.M.; Das, D. Insights into the transport phenomena of iron ore particles by utilizing extracted Bio-surfactant from *Acacia concinna* (Willd.) Dc. *J. Mol. Liq.* **2023**, *382*, 121974. DOI: 10.1016/j.molliq.2023.121974
19. Das, S.N.; Biswal, S.K.; Mohapatra, R.K. Analysing the role of a bio-surfactant extracted from *Colocasia esculenta* (L.) schott on the stabilization of high concentrated iron ore slurry for transportation. *Bull. Chem. Soc. Ethiop.* **2023**, *37*, 1459-1470.
20. Das, S.N.; Biswal, S.K.; Mohapatra, R.K. Exploring the role of a bio-surfactant on the stabilization of high concentrated iron ore slurry. *Rasayan J. Chem.* **2023**, *16*, 1319-1325.
21. Sánchez, M.; González-Burgos, E.; Iglesias, I.; Gómez-Serranillos, M.P. Pharmacological update properties of aloe vera and its major active constituents. *Molecules* **2020**, *25*, 1324.
22. Choi, S.-M.; Supeno, D.; Byun, J.-Y.; Kwon, S.-H.; Chung, S.W.; Kwon, S.-G.; Park, J.-M.; Kim, J.-S.; Kwon, D.-Y.; Choi, W.-S. Chemical characteristics of *Aloe vera* and *Aloe saponaria* in Ulsan Korea. *Int. J. BioSci. Biotechnol.* **2016**, *8*, 109-118.
23. Kamble, S.D.; Gatade, A.A.; Sharma, A.K.; Sahoo, A.K. Physico-chemical composition and mineral content of Aloe vera (*Aloe barbadensis* Miller) gel. *Int. J. Multidisci. Edu. Res.* **2022**, *11*, 73-79.
24. Belbsir, H.; El-Hami, K.; Soufi, A. Modeling and simulation of the flow behavior of the phosphate slurry through the pipeline. *ISTE Open Science* **2017**, *1*, 1-16.
25. Belbsir, H.; El-Hami, K.; Soufi, A. Study of the rheological behavior of the phosphate-water slurry and search for a suitable model to describe its rheological behavior. *Int. J. Mech. Mechatron. Eng.* **2018**, *18*, 73-81.

26. Belbsir, H.; El-Hami, K. *Modeling the Flow Behavior of Phosphate-Water Slurry Through the Pipeline and Simulating the Impact of Pipeline Operating Parameters on the Flow in Advanced Intelligent Systems for Sustainable Development*, Ezziyyani M. (eds.) (AI2SD'2018). AI2SD 2018. *Advances in Intelligent Systems and Computing*, Springer, Cham. **2019**, 912, 357–370. [https://doi.org/10.1007/978-3-030-12065-8\\_3](https://doi.org/10.1007/978-3-030-12065-8_3).
27. Belbsir, H.; El-Hami, K.; Mazouz, H. *Study of the Rheological Behavior of Phosphate Slurry and Its Derivatives Products* in Advanced Intelligent Systems for Sustainable Development Ezziyyani, M. (Ed.) (AI2SD'2019). AI2SD 2019. *Advances in Intelligent Systems and Computing*, Springer: Online Publication; **2020**, 1104, 650-660.
28. Belbsir, H.; El-Hami, K. Adaptation of various explicit formulas for calculating Darcy-Weisbach friction factor to optimize the modeling of pressure drops during turbulent flow of phosphate slurry through the pipeline, *2020 IEEE 6th International Conference on Optimization and Applications (ICOA)*, Beni Mellal, Morocco. **2020**, 1-6. <https://doi.org/10.1109/ICOA49421.2020.9094513>.
29. Shrimali, K.; Jin, J.; Hassas, B.V.; Wang, X.; Miller, J.D. The surface state of hematite and its wetting characteristics. *J. Colloid Interface Sci.* **2016**, 477, 16-24.
30. Rai, S.; Acharya-Siwakoti, E.; Kafle, A.; Devkota, H.P.; Bhattarai, A. Plant-derived saponins: A review of their surfactant properties and applications. *Sci.* **2021**, 3, 44.
31. Patra, A.S.; Makhija, D.; Mukherjee, A.K.; Tiwari, R.; Sahoo, C.R.; Mohanty, B.D. Improved dewatering of iron ore fines by the use of surfactants. *Powder Technol.* **2016**, 287, 43-50.